TELKOMNIKA Telecommunication, Computing, Electronics and Control
Vol. 18, No. 6, December 2020, pp. 3228~3233
ISSN: 1693-6930, accredited First Grade by Kemenristekdikti, Decree No: 21/E/KPT/2018
DOI: 10.12928/TELKOMNIKA.v18i6.13797

Improving optical properties of remote phosphor LED using green $Y_2O_3:Ho^{3+}$ and red $Mg_4(F)(Ge, Sn)O_6:Mn^{2+}$ layers

My Hanh Nguyen Thi[1], Nguyen Thi Phuong Loan[2], Nguyen Doan Quoc Anh[3]
[1]Faculty of Mechanical Engineering, Industrial University of Ho Chi Minh City, Vietnam
[2]Faculty of Fundamental 2, Posts and Telecommunications Institute of Technology, Vietnam
[3]Power System Optimization Research Group, Faculty of Electrical and Electronics Engineering, Ton Duc Thang University, Vietnam

Article Info

Article history:

Received Aug 4, 2019
Revised Apr 6, 2020
Accepted Jul 9, 2002

Keywords:

Color rendering index
Lumen output
$Mg_4(F)(Ge,Sn)O_6:Mn^{2+}$
WLEDs
$Y_2O_3:Ho^{3+}$

ABSTRACT

The lighting device that employs diodes to create white light (WLEDs) with quantum dots (QDs) and phosphor layers is a promising lighting method that is increasingly used in many fields on account of the remarkable color expressing ability. The QDs film is usually placed apart from the phosphor layer according to the packaging configuration to prevent light loss due to backscattering as well as preserve the consistency of the ligands on the QDs surface. The article also conducted experiments to compare the lighting properties and thermal output of the two packaging orders of QDs and phosphor. The heat discharing ranges were simulated with thermography technology, moreover, other parameters such as light energy emission and PL spectra are acquired to evaluate the efficiency of the packaging order. The results from the practical experiment show that while under 10% wt., the luminous output (LO) of green QDs-on-phosphor structure reaches 1130 lm, higher than the red QDs-on-phosphor structure with 878 lm, and the color rendering value in the configuration with red QDs on phosphor is Ra = 74 are higher than Ra = 68 index of the green QDs-on-phosphor structure. As a result, the QDs-on-phosphor is determined as the better packaging configuration to choose to achieve an overall improvement in lighting efficiency, color rendering index

Corresponding Author:

Nguyen Doan Quoc Anh,
Power System Optimization Research Group,
Faculty of Electrical and Electronics Engineering,
Ton Duc Thang University,
Ho Chi Minh City, Vietnam.
Email: nguyendoanquocanh@tdtu.edu.vn

1. INTRODUCTION

White light-emitting diodes (WLEDs) with their phenomenon lighting properties such as high lighting capacity, power saving and excellent endurance are being increasingly utilized in modern lighting applications and flat monitor display [1-3]. Fabricating white light by merging discharged light from the blue chip and the phosphor material $Y_3Al_5O_{12}:Ce^{3+}$ (YAG:Ce) is the most commonly used method. The idea of this method is based on the color-integrating principle, which is combining red and yellow to create white light. While this LEDs model has high lighting efficacy (LE), the red deficiency within the radiation spectrum, which is a much-needed chromatic light to improve the color expression ability, prevents it from obtaining high quality status [4]. Many solutions were suggested in previous researches to address this issue including adding red

phosphor materials to enhance the color rendering ability of pc-LEDs [5-8]. The only problem with this method is the inability of keeping the luminous efficacy index at an acceptable level due to part of their extensive red emitting spectrum exceeds the human perception [9]. The solid-state lighting field in recent time is focusing on the semiconductor quantum dots (QDs), an innovative material that can bring about immense changes to the lighting performance of LEDs, with exceptional optical parameters, namely, the adjustable bandwidth, small emitting range and high quantum productivity [10-13]. The positive effects of QDs on the color rendering index (CRI), color gamut as well as the lighting efficacy of pc-LEDs have been verified both in theory and through practices [14-16]. The most frequently used packaging configurations for pc-LEDs with QDs are applying a compound of QDs and the phosphorous silicone resin or coating the QDs and the phosphor component separately.

The QDs and the phosphor are blended together and put on the LED chip in the first configuration, the combined configuration [17, 18], while in the latter configuration the QDs and phosphor layer are applied individually onto the chip, as separated configuration [19, 20]. The issue with the combined configuration is the QDs in this structure is part of the reflector and, therefore, too close to the LED chip and results in high optical density. The remote structure, on the other hand, with a gap between the QDs sheet and the chip experiences low optical power density. However, the remote structure can stabilize the chemical discrepancy among QDs molecules at the surface and phosphor silicone expoxy by alternating the polymeric condition that the QDs sheet is in [21-23]. With this characteristic, the remote packaging configuration appears to be the optimal solution and was normally applied to create WLEDs with QDs and phosphor.

2. PREPARATION AND SIMULATION

Figure 1 (a) illustrates the scenario where the green QDs particles are placed upon the phosphor layer. Meanwhile, Figure 1 (b) the red QDs lay upon the phosphor layer. The package configuration is a deciding factor to the emitted light and heat radiation, thus deciding the lighting performance of WLEDs. While the relation between the package configuration and the QDs-WLEDs optical performance was thoroughly expressed in previous studies, there was no practical experiment on the transition of lighting power between QDs and phosphor. The findings from said research are an important contribution to the QDs-WLEDs construction guideline, however, the amount of light energy loss during transition in both structures as well as the effect of QDs on the optical performance are the important aspects that have not been discussed.

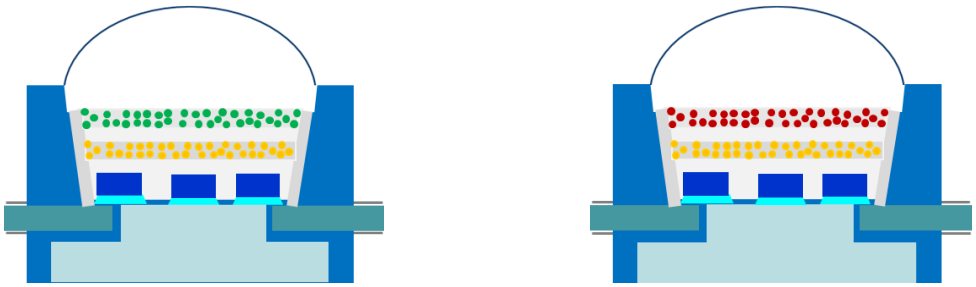

Figure 1. Simulation diagram of two remote WLEDs types with different packaging sequences: (a) green QDs-on-phosphor type, (b) red QDs-on-phosphor type

Therefore, the goal of this article is to gather the information needed for a quantitative research that relates to the aspects mentioned above. The primary method is to analyze the decline of lighting power between QDs and the phosphor layer in both structures, and then compare their operating efficiency to determine which one is the optimal configuration. To serve this experiment, a red emitting QDs CdSe/ZnS and a WLEDs based on yellow emitting phosphor and a band of QDs were created. The emission of lighting energy and PL range indexes needed for the comparison process are computed using an integrating sphere system while the temperature fields on the devices during operation are imitated by putting the optical indexes in thermal simulation and then use an infrared thermal imager to analyze the result. The outcomes from the experiments show that with better lighting efficiency and color rendering index in addition to lower device generated heat, the QDs-on-phosphor is the ideal packaging order to choose for better performance.

3. RESULTS AND DISCUSSION

The results in Figure 2 expressed the different changes occur in terms of concentration between green phosphor Y_2O_3:Ho^{3+}, red phosphor $Mg_4(F)(Ge, Sn)O_6$:Mn^{2+} and yellow phosphor YAG:Ce^{3+}. These changes in concentration affect the ability to absorb or scatter of the phosphor layers in WLEDs, which determine the color quality and the amount of light emitted. Therefore, the concentration setting of the two phosphor layers Y_2O_3:Ho^{3+} and $Mg_4(F)(Ge, Sn)O_6$:Mn^{2+} are extremely important to the optical performance of WLEDs. Moreover, the decreases in the concentration of yellow phosphor YAG:Ce^{3+} corresponding to the increases in concentrations of the Y_2O_3:Ho^{3+} and $Mg_4(F)(Ge, Sn)O_6$:Mn^{2+} is to maintain the average correlated color temperatures. More specifically, YAG:Ce^{3+} concentration decline to preserve the ACCTs when the concentrations of Y_2O_3:Ho^{3+} and $Mg_4(F)(Ge, Sn)O_6$: Mn^{2+} are rising in the range from 2 to 20% wt. The influences of red phosphor $Mg_4(F)(Ge, Sn)O_6$:Mn^{2+} and green phosphor Y_2O_3:Ho^{3+} are expressed in Figure 3. According to Figure 3, the intensity in the range from 420-480 nm and 500 to 640 nm increase with Y_2O_3:Ho^{3+} concentration which confirmed that the luminous flux in these ranges is also increase. Moreover, the scattered blue light also increases, which means the scattering property is improved leading to better correlated color. The advantages that occur when applying the Y_2O_3:Ho^{3+} are notable results that can be utilized to validate the benefit of this green phosphor on the optical properties of WLEDs. In the case of $Mg_4(F)(Ge,Sn)O_6$:Mn^{2+}, the presence of this phosphor cause the intensity from 648 to 738 nm to rise, however, this effect is meaningless without the increase in the two remaining spectrum ranges, which are 420-480 nm and 500-640 nm. Similar to the green phosphor, if the intensity in the remaining spectrums of red phosphor rise that would result in better blue light scattering effect. The emission spectrum that ties to the emitted temperature is crucial in improving the optical performance, particularly, when the emission spectrum increase, the color quality and luminous flux become better. These are important findings when utilizing the red phosphor $Mg_4(F(Ge, Sn)O_6$:Mn^{2+}. The research results show that $Mg_4(F)(Ge, Sn)O_6$:Mn^{2+} guarantee improvement in color quality despite the color temperature, this is a valuable characteristic, especially when maintaining high color quality at high temperature is considered hard to obtain. The final decision relies on the manufacturers to choose the suitable option to reach their goal. For WLEDs that focus on the high chromatic performance, it is advisable to give up a bit of emitted light to achieve highest color quality possible.

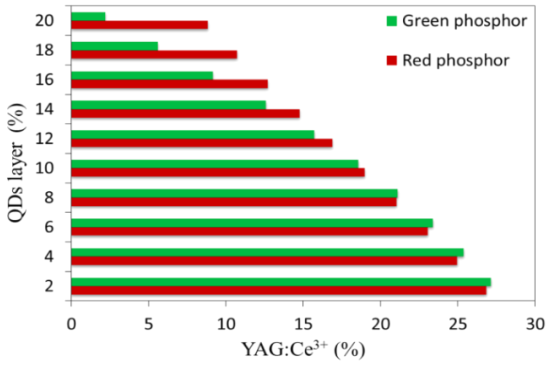

Figure 2. The alteration in phosphor concentration of remote WLEDs to maintain the average CCT

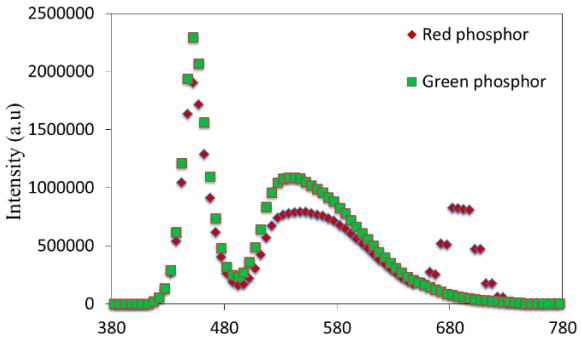

Figure 3. Emission spectra intensity in dual-layer phosphor structures

The CRI expresses the chromatic outcome of the irradiated object. This index denotes the ability to express the color of an object and is based on the balance of blue, yellow, and green. If the proportions of the constituent colors are uneven, the color balance will loss and results in reduced color quality. According to results of CRI presented in Figure 4, the green remote phosphor layer Y_2O_3:Ho^{3+} is detrimental to the CRI. Although the color rendering index decreases slightly whenever there is a green phosphor layer in the structure, this is not a serious defect due to CRI is only part of color quality scale (CQS). The CQS, as can be seen in Figure 5 remain static when the concentration of Y_2O_3:Ho^{3+} is below 8%. In comparison to CRI, the CQS is a priority because it covers more optical properties and is harder to obtain. As a result, it is acceptable to have the concentration of Y_2O_3:Ho^{3+} under 8% if the luminous flux is also appropriate.

The following section is the calculating formula for the unequal SPD of single color LED with Gaussian function [24, 25]:

$$P_\lambda = P_{opt}\frac{1}{\sigma\sqrt{2\pi}}exp\left[-0.5*\frac{(\lambda-\lambda_{peak})^2}{\sigma^2}\right] \quad (1)$$

In this formula, P_λ is the spectral power distribution (SPD) (mW/nm) while λ indicates the wavelength (nm) and λ_{peak} describes the peak wavelength (nm). P_{opt} are used to describe the optical power (W) of the WLED. When σ relies on the peak wavelength λ_{peak}, it is possible to define the full-width at half-maximum (FWHM) $\Delta\lambda$ (nm) as following with λ_1, λ_2 being the wavelengths at half of the peak intensity,h represents Planck's constant (J.s) and c is the speed of light (m.s^{-1}).

$$\sigma = \frac{\lambda_{peak}^2 \Delta E}{2hc\sqrt{2\,ln\,2}} = \frac{\lambda_{peak}^2\left(\frac{hc}{\lambda_1}-\frac{hc}{\lambda_2}\right)}{2hc\sqrt{2\,ln\,2}} = \frac{\lambda_{peak}^2\left(\frac{hc\Delta\lambda}{\lambda_1\lambda_2}\right)}{2hc\sqrt{2\,ln\,2}} \quad (2)$$

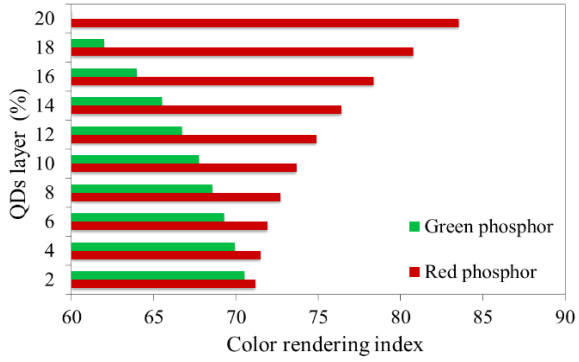

Figure 4. The color rendering index corresponding to the concentration of Y_2O_3:Ho^{3+} and $Mg_4(F)(Ge, Sn)O_6$:Mn^{2+} phosphors

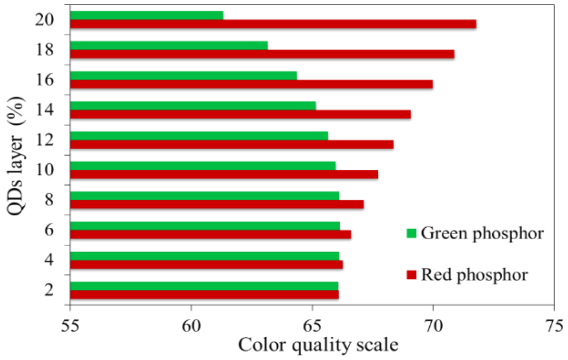

Figure 5. The color quality scale corresponding to the concentration of Y_2O_3:Ho^{3+} and $Mg_4(F)(Ge, Sn)O_6$:Mn^{2+} phosphors

In theory, WLED with YAG phosphor and blue light emitting chip has the combination between blue and yellow spectra as SPD. In practical experiment, yellow phosphor actually active in both yellow and green emission ranges. With that being said, it is possible to use the green spectrum to depict the discrepancy between the SPD in practice and blue-yellow mixed spectrum in cases with blue and yellow are the chosen spectra. As a result, the green spectrum is added to the model for practical circumstances and the analytical tri-spectrum (B-G-Y) is expressed as in (3) then later on modified to (4):

$$P_\lambda = P_{opt\_b}\frac{1}{\sigma_b\sqrt{2\pi}}exp\left[-0.5*\frac{(\lambda-\lambda_{peak\_b})^2}{\sigma_b^2}\right]$$

$$P_{opt_g}\frac{1}{\sigma_g\sqrt{2\pi}}exp\left[-0.5*\frac{(\lambda-\lambda_{peak_g})^2}{\sigma_g^2}\right] \quad (3)$$

$$P_{opt\_y}\frac{1}{\sigma_y\sqrt{2\pi}}exp\left[-0.5*\frac{(\lambda-\lambda_{peak\_y})^2}{\sigma_y^2}\right]$$

$$P_\lambda = \eta_b P_{opt_{total}}\frac{1}{\sigma_b\sqrt{2\pi}}exp\left[-0.5*\frac{(\lambda-\lambda_{peak_b})^2}{\sigma_b^2}\right]$$

$$\eta_g P_{opt_{total}}\frac{1}{\sigma_g\sqrt{2\pi}}exp\left[-0.5*\frac{(\lambda-\lambda_{peak_g})^2}{\sigma_g^2}\right]$$

$$\eta_y P_{opt\_total}\frac{1}{\sigma_y\sqrt{2\pi}}exp\left[-0.5*\frac{(\lambda-\lambda_{peak\_y})^2}{\sigma_y^2}\right] \quad (4)$$

where P_{opt_b}, P_{opt_g}, $P_{opt_y}$and P_{opt_total} stand for the optical power (W) in each separate spectrum of blue, green, yellow and white. λ_{peak_b}, λ_{peak_g} and λ_{peak_y}in order are the peak wavelengths (nm) of the spectra

emitting the chromatic lights. The non-dimensional ratios of chromatic lights spectra to the range of white light, are expressed respectively as η_b, η_g and η_y. σ_b, σ_g and σ_y in turn are the coefficient of FWHM (nm) for the wavelength ranges of chromatic lights. This mathematical models for SPC in WLEDs with phosphor layer can be perceived as a tricolor spectrum and an extended Gaussian model. Next, we study the luminous flux of QDs WLED with the QDs concentration as in Figure 6.

The content of Figure 6 demonstrates that when the concentration range of Y_2O_3:Ho^{3+} is from 2% wt to 20% wt the luminous will sharply increase. However, the luminous flux in remote phosphor structure with dual layers is a result of both phosphor layers including the red phosphor $Mg_4(F)(Ge, Sn)O_6$:Mn^{2+}. The extinction coefficient increase with $Mg_4(F)(Ge, Sn)O_6$:Mn^{2+} concentration while opposing to light transmission energy as the application of Beer's Law suggests. Therefore, when choosing the concentration for the phosphor layers it may occur the lumen output decreases when the concentration of $Mg_4(F)(Ge, Sn)O_6$:Mn^{2+} increases, and drastically decline especially when the concentration reaches 20%. Despite the drawback in luminous flux, using red phosphor $Mg_4(F)(Ge,Sn)O_6$:Mn^{2+} is still beneficial because of the enhancements it brings to the CRI and CQS, not to mention the luminous flux in these dual-layer phosphor structures is better than the single-layer ones that do not have a red phosphor layer. These references help the manufacturers choose the exact concentration of the phosphor to serve their purpose in mass production.

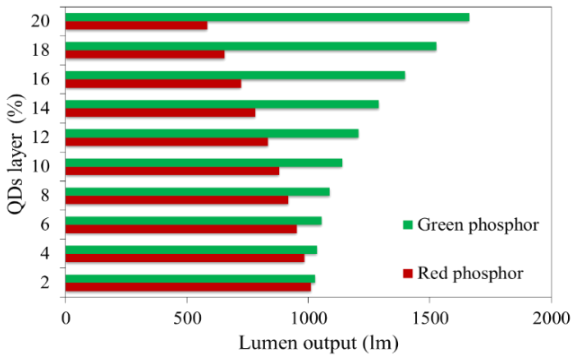

Figure 6. The luminous flux corresponding to the concentration of Y_2O_3:Ho^{3+} and $Mg_4(F)(Ge, Sn)O_6$:Mn^{2+} phosphors

4. CONCLUSION

The results of this research paper confirmed the benefits of green phosphor Y_2O_3:Ho^{3+} and red phosphor $Mg_4(F)(Ge, Sn)O_6$:Mn^{2+} on the optical properites of remote structure with two phosphor layers. Through the study of scattering characteristic with scattering theory and the Beer's law, it is confirmed that the red phosphor $Mg_4(F)(Ge, Sn)O_6$: Mn^{2+} is capable of boosting the chromatic quality. On the other hand, the green phosphor Y_2O_3:Ho^{3+} is the excellent substance to improve the luminous flux, the effect is not only applicable to low color temperature WLEDs but also with the ones at high color temperature. With the aforementioned results, this research has succeeded in a very difficult task that is enhancing the color quality in remote phosphor structure. On another note, the concentration of both phosphor layers Y_2O_3:Ho^{3+} or $Mg_4(F)(Ge, Sn)O_6$:Mn^{2+} must be kept at an appropriate level as the excessive amount of phosphor can damage the color quality as well as the luminous flux. Managing the concentration of phosphor is crucial in producing WLEDs, however, this article has presented all the much-needed information about this topic to the manufacturers so they can apply it to create WLEDs with the desired quality.

REFERENCES

[1] S. Sadeghi, *et al.*, "Quantum dot white LEDs with high luminous efficiency," *Optica*, vol. 5, no. 7, pp. 793-802, 2018.
[2] X. Kong, *et al.,* "Assessing the temporal uniformity of CIELAB hue angle," *Journal of the Optical Society of Amerika A,* vol. 37, no. 4, pp. 521-528, March 2020.
[3] X. Li, *et al.*, "Single-shot multispectral imaging through a thin scatterer," *Optica*, vol. 6, pp. 864-871, 2019.
[4] S. Pan, *et al.*, "Image restoration and color fusion of digital microscopes," *Applied Optics*, vol. 58, no. 9, pp. 2183-2189, March 2019.
[5] B. K. Tsai, *et al.,* "Exposure study on UV-induced degradation of PTFE and ceramic optical diffusers," *Applied Optics*, vol. 58, no. 5, pp. 1215-1222, February 2019.

[6] X. Wang, *et al.*, "Modifying phase, shape and optical thermometry of NaGdF4:2%Er^{3+}phosphors through Ca^{2+} doping," *Opt. Express,* vol. 26, no. 17, pp. 21950-21959, August 2018.
[7] X. Fu, *et al.,* "Micromachined extrinsic Fabry-Pérot cavity for low-frequency acoustic wave sensing," *Optics Express,* vol. 27, no. 17, pp. 24300-24310, August 2019.
[8] A. Ullah, *et al.,* "Household light source for potent photo-dynamic antimicrobial effect and wound healing in an infective animal model," *Biomed. Opt. Express,* vol. 9, no. 3, pp. 1006-1019, March 2018.
[9] D. Durmus, *et al.*, "Blur perception and visual clarity in light projection systems," *Opt. Express,* vol. 27, no. 4, pp. A216-A223, February 2019.
[10] A. Lihachev, *et al.*, "Differentiation of seborrheic keratosis from basal cell carcinoma, nevi and melanoma by RGB autofluorescence imaging," *Biomedical Optical Express*, vol. 9, no. 4, pp. 1852-1858, April 2018.
[11] J. Zhou, *et al.*, "Low-voltage wide-field-of-view lidar scanning system based on a MEMS mirror," *Applied Opt*ics, vol. 58, no. 5, pp. A283-A290, 2019.
[12] J. S. Li, *et al.*, "High efficiency solid–liquid hybrid-state quantum dot light-emitting diodes," *Photonics Research,* vol. 6, no. 12, pp. 1107-1115, December 2018.
[13] S. Lee, *et al.*, "Printed cylindrical lens pair for application to the seam concealment in tiled displays," *Optics Express,* vol. 26, no. 2, pp. 824-834, January 2018.
[14] H. Yuce, *et al.,* "Phosphor-based white LED by various glassy particles: control over luminous efficiency," *Optics Letters*, vol. 44, no. 3, pp. 479-482, February 2019.
[15] Q. Zhang, *et al*., "Excellent luminous efficiency and high thermal stability of glass-in-LuAG ceramic for laser-diode-pumped green-emitting phosphor," *Optiics Letters*, vol. 43, no. 15, pp. 3566-3569, August 2018.
[16] V. Fuertes, *et al*., "Enhanced luminescence in rare-earth-free fast-sintering glass-ceramic," *Optica*, vol. 6, no. 5, pp. 668-679, May 2019.
[17] X. Huang, *et al.,* "High-brightness and high-color purity red-emitting Ca3Lu, AlO.3, BO3.4: Eu3+phosphors with internal quantum efficiency close to unity for near-ultraviolet-based white-light-emitting diodes," *Optics Letters*, vol. 43, no. 6, pp. 1307-1310, 2018.
[18] W. Gao, *et al.,* "Color temperature tunable phosphor-coated white LEDs with excellent photometric and colorimetric performances," *Applied Optics*, vol. 57, no. 31, pp. 9322-9327, November 2018.
[19] H. L. Ke, *et al.*, "Lumen degradation analysis of LED lamps based on the subsystem isolation method," *Applied Optics,* vol. 57, no. 4, pp. 849-854, February 2018.
[20] S. Beldi, *et al.*, "High Q-factor near infrared and visible Al2O3-based parallel-plate capacitor kinetic inductance detectors," *Opt. Express,* vol. 27, no. 9, pp. 13319-13328, April 2019.
[21] H. Liu, *et al.,* "Design of a six-gas NDIR gas sensor using an integrated optical gas chamber," *Optics Express,* vol. 28, no. 8, pp. 11451-11462, March 2020.
[22] D. Lu, *et al.,* "Synthesis and photoluminescence characteristics of the LiGd3, MoO4.5: Eu3+red phosphor with high color purity and brightness," *Optical Materials Express,* vol. 8, no. 2, pp. 259-269, February 2018.
[23] L. Wu, *et al*., "Hybrid warm-white organic light-emitting device based on tandem structure," *Optics Express,* vol. 26, no. 26, pp. A996-A1006, December 2018.
[24] S. Elmalem, *et al.,* "Learned phase coded aperture for the benefit of depth of field extension," *Optics Express,* vol. 26, no. 12, pp. 15316-15331, June 2018.
[25] J. H. Kim, *et al.,* "Synthesis of Mn-doped CuGaS2 quantum dots and their application as single downconverters for high-color rendering solid-state lighting devices," *Optical Materials Express,* vol. 8, no. 2, pp. 221-230, February 2018.